Hindawi
Geofluids
Volume 2021, Article ID 6662809, 12 pages
https://doi.org/10.1155/2021/6662809

Research Article

Prediction of Vibration Velocity of Bench Blasting Reflecting Negative Elevation Effect

Xiaojun Zhang[1,2] **and Jianjun Shi**[1]

[1]*Beijing Key Laboratory of Urban Underground Space Engineering, School of Civil and Resource Engineering, University of Science and Technology Beijing, Beijing 100083, China*
[2]*College of Architecture and Civil Engineering, Beijing University of Technology, Beijing 100124, China*

Correspondence should be addressed to Jianjun Shi; keyan@ces.ustb.edu.cn

Received 9 December 2020; Revised 29 December 2020; Accepted 13 January 2021; Published 3 February 2021

Academic Editor: Bin Gong

In the field of mine blasting practice, accurate prediction of blasting vibration is considered as a critical task. In accordance with the theory of elastic wave, the reflection of blasting vibration wave at the interface of negative elevation is analyzed in this paper. The negative elevation effect exerted by blasting vibration is interpreted considering the mechanism, and the formula of the blasting vibration prediction step (negative) $V = K(Q^{1/3}/R)^{\alpha} \cdot (1/H)^{\beta}$ is derived, reflecting the negative elevation effect. Besides, the formula accuracy is verified by the measured vibration velocity of the mass in the Jinou coal mine. The step (negative) formula acts as a more feasible candidate for the prediction of step blasting vibration.

1. Introduction

In large-scale deep open pits, the blasting scale is large on the whole, and the blasting operations are relatively frequent. Accordingly, the vibration effect exerted by blasting is a critical factor affecting the safety of blasting and the mass stability of slope rock. Thus, the blasting vibration effect predicted accurately lays a basis for controlling the blasting vibration effect. Such prediction is a vital task in the practice of mine blasting, as well as a crucial problem in the research of the technology for blasting vibration control.

In the blasting for strip mining, the elevation effect attributed to the blasting vibration wave propagation along the slope of the stope is considered in the study of the law of vibration attenuation. In recent years, the elevation effect of blasting vibration has been extensively studied in-depth. According to the studies by Lü et al. [1], the convex surface above the source can significantly amplify the blasting vibration. Besides, the larger the height difference, the more obvious the blasting vibration will be amplified. Shu et al. [2] found that the amplifying effect of elevation is associated with the slope. When the slope ratio is above 1/2, the slope will lead to the amplification of the elevation; otherwise, there will be no amplifying effect. Tang and Li [3] considered that the open pit slope can amplify the blasting vibration of the explosion source underneath the foot of the slope, and the vibration speed is upregulated unevenly with the rise in the height. When the critical height is reached, the amplification factor will reach its peak. When the height rises further, the amplification factor will gradually decrease. Chen et al. [4] considered that the amplifying effect of elevation on the blasting vibration in an open pit is affected by the shape of the slope and the dynamic load of the blasting. When the slope rises, or when the shape varies, the vibration intensity of the upper step may be greater than that of the lower step. Through experimental observation and analysis, Wan et al. [5] considered that the amplifying effect of the step terrain blasting vibration is affected by the whiplash effect and the slope effect. Zhang et al. [6], Hu et al. [7], and Zhou and Li [8] analyzed the physical quantities associated with blasting vibration. Then, they conducted the dimensional analysis to derive the blasting vibration formula reflecting the amplifying effect of elevation and applied it in engineering. In the meantime, the dynamic finite element method was

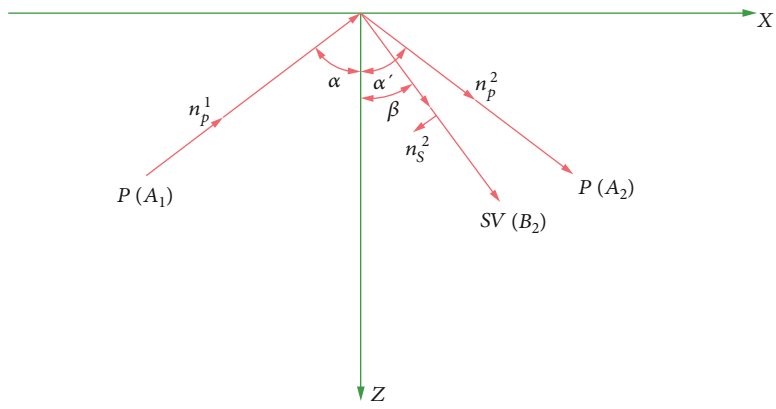

Figure 1: P wave incidence.

successfully introduced in the blasting dynamic simulation, and it was proved that the vibration velocity of the particle at the top of the slope exerts an amplifying effect [9]. The amplification phenomenon is reflected as a local dynamic response [10–18]. However, most of the above studies on elevation effects were conducted by field monitoring and using numerical models. The studies on the mechanism of the elevation effect have been mostly the qualitative description. The blasting vibration prediction formulas using the dimensional analysis are different in form, exhibiting poor theoretical stringency, and the elevation effect cannot be explained from the mechanism. In accordance with the theory of elastic wave, the reflection of blasting vibration wave at the interface of negative elevation is studied in this paper from the angle of blasting vibration elastic wave, and the negative elevation effect of blasting vibration from its mechanism is explained. The blasting vibration step (negative) prediction formula reflecting the negative elevation effect was proposed in this study, and the accuracy of the formula was verified by the actual measured particle vibration velocity in Jinou open-pit coal mine.

2. Mechanism Analysis of Negative Elevation Effect of Blasting Vibration

It is assumed that the underground rock formation is isotropic and the explosion source is spherically symmetric. Blasting seismic waves propagate in the formation in the form of spherical waves. At the same time, the ground is assumed to be a free surface. After the seismic waves reach the ground, they are reflected and superimposed on the ground. By comparing the reflection of the flat ground model and the step model on the free surface, the negative elevation effect of blasting vibration is explained. The main theory used here is the theory of elastic spherical wave propagation in uniform and isotropic media. There is also the reflection theory of elastic waves on free surfaces. In the process of elastic wave reflection analysis on free surface, a representative longitudinal (P) wave is analyzed.

2.1. Propagation of Blasting Vibration Elastic Wave. The seismic wave attributed to blasting refers to an elastic wave propagating in a subterranean formation [19], so the source of the explosion is assumed to be spherically symmetric. When the seismic wave propagates inside the rock mass and does not reach the ground, it can be considered a divergent spherical wave. If the spherical wave consists of a P wave component and a S wave component, set u_p, u_s as the displacement field, respectively, and φ and ψ still represent the potential of the displacement field, and

$$u = u_p + u_s = \nabla_\varphi + \nabla \times \psi. \tag{1}$$

Take the P wave as an example. It yields

$$\varphi = \frac{A}{r} \exp\left[i(kr - wt)\right], \quad r > 0. \tag{2}$$

The displacement vector field is defined as

$$u_p = \nabla\varphi = \frac{\partial\varphi}{\partial r} e_r = A\left(\frac{ik}{r} - \frac{1}{r^2}\right) \exp\left[i(kr - wt)\right] e_r, \tag{3}$$

where A denotes the amplitude of ψ at the source, equal to a constant; w is the circular frequency of the wave; $k = w/c = 2\pi/\lambda$ represents the circular wave number; r is the distance from the observation point to the source. When $r >> \lambda$, $1/\lambda \geq 1/r$. Because two of the brackets in Equation (3) are known, $1/r^2$ can be omitted. Then, Equation (3) is written as

$$u_p = \frac{ikA}{r} \exp\left[i(kr - wt)\right] e_r. \tag{4}$$

Equation (4) expresses the simple harmonic of the spherical displacement, indicating that the amplitude of the displacement at a distance away from the source is inversely proportional to the distance from the source.

The magnitude of the wave displacement can be calculated by the above equation:

$$u_p = \frac{A}{r} e^{i(kr - wt)}. \tag{5}$$

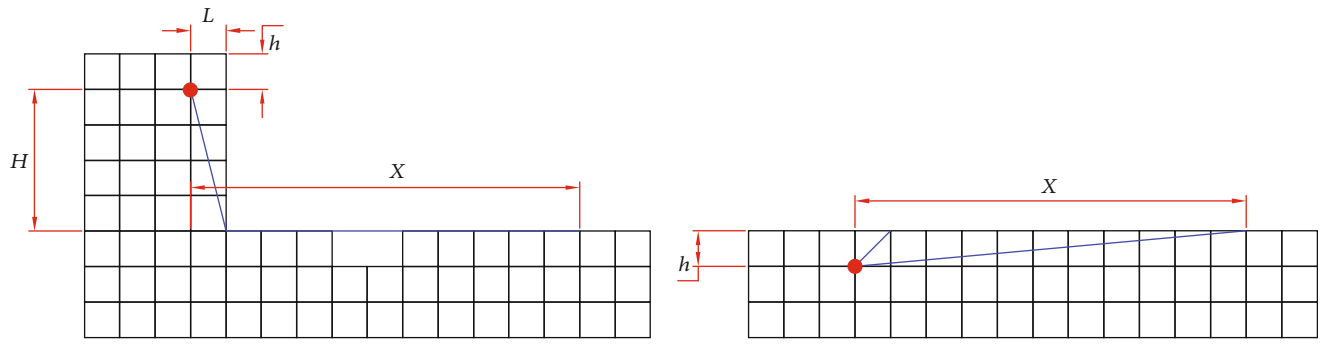

(a) Step model (b) Flat model

Figure 2: Elastic wave propagation model.

The above equation was used to derive the time, i.e., the particle velocity at the observation point is expressed as

$$C_p = -w\frac{A}{r}e^{i(kx-wt)}. \tag{6}$$

2.2. Reflection of Elastic Waves on Free Surfaces. The free surface acts as a special interface, i.e., the boundary between the medium and the vacuum. Thus, there exists no medium on one side of the interface. In practice, the earth is commonly considered a free surface [20]. Figure 1 shows that taking the x-y plane as a free surface, a P wave is incident from the lower medium onto the free surface. Since there exists no medium on the surface, when the wave reaches the boundary of the medium, it can only fold back into the original medium to propagate without passing through it, i.e., there is only a reflected wave rather than a transmitted wave. When the P wave is incident on the free surface, it will cause the displacement along the normal direction of the surface and along the tangential direction. Thus, the reflected wave consists of both P wave and SV wave. In the meantime, according to the symmetry of the problem and the independence of the P wave, the SV wave, and the SH wave, the reflected wave contains no SH wave component (e.g., the incident wave).

The displacement vectors of the incident P wave, the reflected P wave, and the reflected SV wave are expressed as

$$\left.\begin{aligned}
\vec{s}_p^{\,1} &= j\frac{w}{V_p}A_1 e^{j(k_x x+k_z z-wt)}\vec{n}_p^{\,2}\\
\vec{s}_p^{\,2} &= j\frac{w}{V_p}A_2 e^{j\left(k_x' x+k_z' z-wt\right)}\vec{n}_p^{\,2}\\
\vec{s}_s^{\,2} &= j\frac{w}{V_s}B_2 e^{j\left(k_x'' x+k_z'' z-wt\right)}\vec{n}_S^{\,2}
\end{aligned}\right\}, \tag{7}$$

where w denotes the circular frequency of the wave; V_P and V_S are the speeds of P and S waves, respectively; A_1, A_2, B_2 are the amplitude of each wave function; $\vec{n}_p^{\,1}$, $\vec{n}_p^{\,2}, \vec{n}_s^{\,2}$ represent the unit vector of the displacement direction of the wave.

In accordance with the propagation law of the elastic wave at the interface, on the free surface $z = 0$, the magnitude of the displacement of each wave is expressed as

$$\left.\begin{aligned}
s_p^{\,1} &= \frac{w}{V_p}A_1 e^{j(k_x x-wt)}\\
s_p^{\,2} &= \frac{w}{V_p}A_2 e^{j(k_x x-wt)}\\
s_s^{\,2} &= \frac{w}{V_s}B_2 e^{j(k_x x-wt)}
\end{aligned}\right\}. \tag{8}$$

The above displacement formula was adopted to calculate the time t, and the calculated velocity of the particle at the observation point of each wave is expressed as follows:

$$\left.\begin{aligned}
C_p^{\,1} &= -\frac{w^2}{V_p}A_1 e^{j(k_x x-wt)}\\
C_p^{\,2} &= -\frac{w^2}{V_p}A_2 e^{j(k_x x-wt)}\\
C_s^{\,2} &= -\frac{w^2}{V_s}B_2 e^{j(k_x x-wt)}
\end{aligned}\right\}. \tag{9}$$

Based on the geometric relationship, the reflected P wave and the reflected SV wave are superimposed on each other at the free surface, and the velocity in the x-direction and the z-direction is expressed as

$$\left.\begin{aligned}
C_x &= C_p^{\,2}\sin a - C_s^{\,2}\cos\beta\\
C_z &= C_p^{\,2}\cos a + C_s^{\,2}\sin\beta
\end{aligned}\right\}. \tag{10}$$

2.3. Mechanism Analysis of Negative Elevation Effect of Step Blasting Vibration. To study the negative elevation effect mechanism of step blasting vibration, a geometric model was built, as shown in Figure 2. Assume that the step model exhibits a high steep shape, there is a certain distance of the observation point from the explosion source, and the depth of the explosive is relatively shallow. In the step model, the distance between the blasthole and

the edge of the step is almost equal to the depth of the explosive. The depth of the medicine package is denoted as h, the step height is H, the distance from the medicine bag to the edge of the step is l, and the horizontal distance of the observation point from the drug pack is x. According to the Huygens-Fresnel principle [21], each point on the wavefront (wave front) can be considered the wave source of the transmitted wavelet in the propagation process. At any subsequent time, the envelope surface of these wavelets can act as a new wavefront. The envelope surface is formed by the interference of the wavelets generated by the points on the wavefront at the observation points. In the meantime, based on the Fermat principle [22], the wave always propagates along the path with the smallest propagation time in the medium. These paths are rays, and the rays are straight lines in a uniform medium. Subsequently, from the explosion source to the observation point E at the same horizontal distance from the explosion source, the seismic wave propagation in the step model follows the path of $O-D-E$, and the path propagated in the flat model is $O-E$ (where O denotes the center of the explosion source), as shown in Figure 2.

According to Equation (10), in the step model, after the elastic waves are superposed on each other at the free surface E, the particle velocity of the point can be, respectively, expressed in the X-direction and the Z-direction as follows:

$$\left.\begin{aligned} C_{x1} &= {C_p}^{2\prime} \sin a_1 - {C_s}^{2\prime} \cos \beta_1 \\ C_{z1} &= {C_p}^{2\prime} \cos a_1 + {C_s}^{2\prime} \sin \beta_1 \end{aligned}\right\}. \tag{11}$$

In the flat model, after the elastic waves are superimposed on each other at the free surface E, the velocity of the point particle is expressed, respectively, in the X -direction and the Z-direction as follows:

$$\left.\begin{aligned} C_{x2} &= {C_p}^{2\prime\prime} \sin a_2 - {C_s}^{2\prime\prime} \cos \beta_2 \\ C_{z2} &= {C_p}^{2\prime\prime} \cos a_2 + {C_s}^{2\prime\prime} \sin \beta_2 \end{aligned}\right\}, \tag{12}$$

where α_1, β_1 denote the incident angles and reflection angles of the waves at a certain point in the step model. α_2, β_2 represent the incident angle and reflection angle of the wave at a certain point in the flat model, respectively.

In the step model, compared with the flat model, the vibration velocity magnification in the X-direction and the Z-direction is expressed as

$$R_{cxT} = \frac{C_{x1}}{C_{x2}}, \tag{13}$$

$$R_{czT} = \frac{C_{z1}}{C_{z2}}. \tag{14}$$

Substituting Equations (11) and (12) into the above equations, they are simplified according to Equation (9) as

$$\begin{aligned} R_{cxT} &= \frac{{A_2}' \sin \alpha_1 - \left(V_p/V_s\right){B_2}' \cos \beta_1}{{A_2}'' \sin a_2 - \left(V_p/V_s\right){B_2}'' \cos \beta_2} \\ &= \frac{{A_1}'}{{A_1}''} \frac{\left({A_2}'/{A_1}'\right) \sin \alpha_1 - \left(V_p/V_s\right)\left({B_2}'/{A_1}'\right) \cos \beta_1}{\left({A_2}''/{A_1}''\right) \sin a_2 - \left(V_p/V_s\right)\left({B_2}''/{A_1}''\right) \cos \beta_2}, \end{aligned} \tag{15}$$

$$\begin{aligned} R_{czT} &= \frac{{A_2}' \cos a_1 + {B_2}'\left(V_p/V_s\right) \sin \beta_1}{{A_2}'' \cos a_2 + {B_2}''\left(V_p/V_s\right) \sin \beta_2} \\ &= \frac{{A_1}'}{{A_1}''} \frac{\left({A_2}'/{A_1}'\right) \cos a_1 + \left({B_2}'/{A_1}'\right)\left(V_p/V_s\right) \sin \beta_1}{\left({A_2}''/{A_1}''\right) \cos a_2 + \left({B_2}''/{A_1}''\right)\left(V_p/V_s\right) \sin \beta_2}, \end{aligned} \tag{16}$$

where ${A_2}'/{A_1}'$, ${B_2}'/{A_1}'$, ${A_2}''/{A_1}''$, and ${B_2}''/{A_1}''$ denote P wave and SVwave reflection coefficients, respectively.

$$\left.\begin{aligned} \frac{{A_2}'}{{A_1}'} &= \frac{{V_s}^2 \sin 2\alpha_1 \sin 2\beta_1 - {V_p}^2 \cos^2 2\beta_1}{{V_s}^2 \sin 2\alpha_1 \sin 2\beta_1 + {V_p}^2 \cos^2 2\beta_1} \\ \frac{{B_2}'}{{A_1}'} &= \frac{-2{V_s}^2 \sin 2a_1 \cos 2\beta_1}{{V_S}^2 \sin 2a_1 \sin 2\beta_1 + {V_p}^2 \cos^2 2\beta_1} \end{aligned}\right\}, \tag{17}$$

$$\left.\begin{aligned} \frac{{A_2}''}{{A_1}''} &= \frac{{V_s}^2 \sin 2\alpha_2 \sin 2\beta_2 - {V_p}^2 \cos^2 2\beta_2}{{V_s}^2 \sin 2\alpha_2 \sin 2\beta_2 + {V_p}^2 \cos^2 2\beta_2} \\ \frac{{B_2}''}{{A_1}''} &= \frac{-2{V_s}^2 \sin 2a_2 \cos 2\beta_2}{{V_S}^2 \sin 2a_2 \sin 2\beta_2 + {V_p}^2 \cos^2 2\beta_2} \end{aligned}\right\}. \tag{18}$$

In the step model, according to Equation (6), the velocity of the particle at the observation point E (where the elastic wave does not reach the critical point of the free surface) is expressed as

$${C_{p1}}' = -w \frac{A}{\sqrt{(H-h)^2 + l^2} \times (x-l)} e^{i(kr-wt)}. \tag{19}$$

Subsequently, the amplitude of the particle vibration velocity is expressed as

$${A_1}' = -w \frac{A}{\sqrt{(H-h)^2 + l^2} \times (x-l)}. \tag{20}$$

In the flat model, according to Equation (6), the velocity of the particle at the observation point E (where the elastic wave does not reach the critical point of the free surface) is expressed as

$${C_{p1}}'' = -w \frac{A}{\sqrt{h^2 + x^2}} e^{i(kr-wt)}. \tag{21}$$

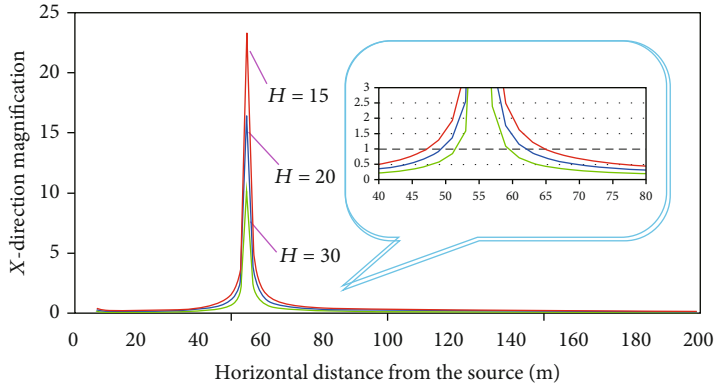

Figure 3: X-direction particle vibration speed magnification.

Next, its amplitude of particle vibration velocity is expressed as

$$A_1'' = -w\frac{A}{\sqrt{h^2 + x^2}}. \tag{22}$$

Then,

$$\frac{A_1'}{A_1''} = \frac{\sqrt{h^2 + x^2}}{\sqrt{(H-h)^2 + l^2} \times (x - l)}. \tag{23}$$

The relationship between the velocity ratio of elastic longitudinal wave and transverse wave and Poisson's ratio v is defined as [23]

$$\frac{V_p}{V_s} = \sqrt{\frac{2(1-v)}{1-2v}}. \tag{24}$$

In accordance with Snell's law [24], it yields

$$\frac{V_p}{V_s} = \frac{\sin a}{\sin \beta}. \tag{25}$$

Set

$$\left.\begin{array}{l} v = 0.25 \\ h = 5 \\ l = 5 \end{array}\right\}. \tag{26}$$

According to the relationship between Equations (15) and (16) and other parameters, through the MATLAB math software drawing, the relationships between the X-direction and Z-direction magnification and the horizontal distance and vertical distance from the explosion source were plotted, as shown in Figures 3 and 4, respectively.

Figure 3 shows that the magnification of the vibration velocity in the X-direction is above 1, and the remaining magnifications are all no less than 1, at a horizontal distance of 50-65 m from the source of the explosion. Accordingly, the existence of the negative elevation of the step model is primarily reflected in the decreasing effect on the vibration velocity. Figure 4 shows the Z-direction particle vibration velocity magnification is extremely small, almost zero. This reveals that the vibration velocity of the particle is significantly downregulated because of the existence of the negative elevation of the step model. In the meantime, Figure 4 suggests that the larger the step negative elevation, the smaller the amplification factor of the vibration speed will be. Figures 3 and 4 indicate that the magnification of the vibration velocity of the step negative elevation is inevitably associated with the horizontal distance and the elevation difference.

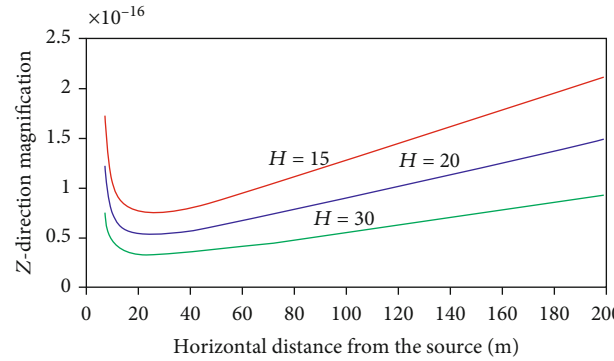

Figure 4: Z-direction particle vibration speed magnification.

3. Prediction Formula of Blasting Vibration Velocity Reflecting Negative Elevation Effect

From the above, the vibration velocity ratio of the measuring points with equal horizontal distance and different vertical distance is obtained, but it is more complicated and needs to be simplified. Then, combined with the Sadowski formula, the vibration velocity prediction formula reflecting the negative elevation effect was deduced.

3.1. Negative Elevation Effect Magnification Analytic Simplification. In large-scale deep open pits, the general step slope is relatively high and steep. Besides, there is a certain

distance of the observation point from the source. Also, the analytical formula of the negative elevation effect magnification is further approximated according to the assumptions of the step model and the flat model.

The table shows that Poisson's ratio v varies by $0 \sim 0.5$, and the general Poisson's ratio v of rock is around 0.25. It yields

$$v = 0.25. \tag{27}$$

In the step model, $\alpha_1 = 90^\circ$, so it yields

$$\left.\begin{aligned} \beta_1 &= 35.27^\circ \\ \frac{A_2}{A_1} &= -1 \\ \frac{B_2}{A_1} &= 0 \end{aligned}\right\}. \tag{28}$$

In the flat model, the burial depth h of the blasthole is smaller than the distance X of the observation point from the center of the explosion source. Assume $h < 6h \leq x$.

Subsequently, the range of the P wave incident angle α_2 is $81^\circ \leq \alpha_2 < 90^\circ$.

Since the value of α_2 varies slightly, to simplify the calculation, set $\alpha_2 = 86^\circ$. Then, it yields

$$\left.\begin{aligned} \beta_2 &= 35.17^\circ \\ \frac{A_2{}'}{A_1{}'} &= -0.4431 \\ \frac{B_2{}'}{A_1{}'} &= -0.1990 \end{aligned}\right\}. \tag{29}$$

According to the conditions of the initial hypothesis, the step is high, and there is a certain distance of the observation point from the source. Thus, the depth of the explosive is smaller than the distance from the observation point to explosive source, which is negligible. Furthermore, the distance between the depth of the explosive is nearly equal to the length of the blasthole from the edge of the step, which is expressed as

$$h \approx l. \tag{30}$$

Then,

$$\frac{A_1}{A_1{}'} \approx \frac{\sqrt{h^2 + x^2}}{\sqrt{(H-h)^2 + h^2} \times (x-h)} \approx \frac{x}{\sqrt{(H-h)^2 + h^2} \times x}. \tag{31}$$

Because the step is high steep, and the depth of the explosive is associated with the elevation difference H, which is relatively small, the depth is neglected and further simplified as

$$\frac{A_1}{A_1{}'} \approx \frac{x}{\sqrt{H^2} \times x} = \frac{1}{H}. \tag{32}$$

Substituting Equations (27), (28), (29), and (32) into Equations (15) and (16), it yields

$$R_{cxT} = 6.2\left(\frac{1}{H}\right), \tag{33}$$

$$R_{czT} = 0 \cdot \left(\frac{1}{H}\right). \tag{34}$$

Equations (33) and (34) are unified, and the parameter k_1 is introduced, i.e., the amplification factor R_{cT} of the step model negative acceleration vibration speed is expressed as

$$R_{cT} = k_1 \cdot \left(\frac{1}{H}\right). \tag{35}$$

To reduce the error caused by the approximation during the above simplification, the parameter β was introduced, and Equation (35) is written as

$$R_{cT} = k_1 \cdot \left(\frac{1}{H}\right)^{\beta}. \tag{36}$$

3.2. Prediction Formula of Vibration Velocity Reflecting Negative Elevation Effect. The vibration velocity at the blasting observation point of the negative elevation step model is denoted as V_1. According to the Sadowski formula, the formula for predicting the vibration velocity of the observation point widely used in flat terrain is written as [22]

$$V = k\left(\frac{Q^{1/3}}{R}\right)^{\alpha}, \tag{37}$$

where V is the ground particle peak vibration velocity, cm/s; Q is the explosive quantity (the total charge amount when bursting together, the maximum charge amount when delaying blasting), kg; R is the distance from the observation point to the source, m; k, α are the coefficient and attenuation coefficient associated with the topography and geological conditions between the blasting point and the calculation point.

Subsequently, the vibration speed V_1 of the negative elevation step model was compared with the vibration speed of the flat terrain, and the magnification is expressed as

$$R_{cT} = \frac{V_1}{V}. \tag{38}$$

Table 1: Measurement point blasting vibration monitoring data.

Data	Dose (kg)	Number	Distance		Velocity (cm/s)	Data	Dose (kg)	Number	Distance		Velocity (cm/s)
			Level	Vertical					Level	Vertical	
		1	126	-36.4	0.986			1	65	-1.7	19.624
		2	172	-36.4	1.061			2	83	-1.7	16.696
		3	182	-62.3	0.927			3	100	-22.7	2.906
Oct 15th	255.81	4	193	-62.3	1.107	Oct 16th	255.81	4	117.7	-22.7	4.163
		5	252	-72.4	0.458			5	141.4	-45	1.108
		6	316	-72.4	0.266			6	168.6	-45	1.114
								7	195	-45	0.96

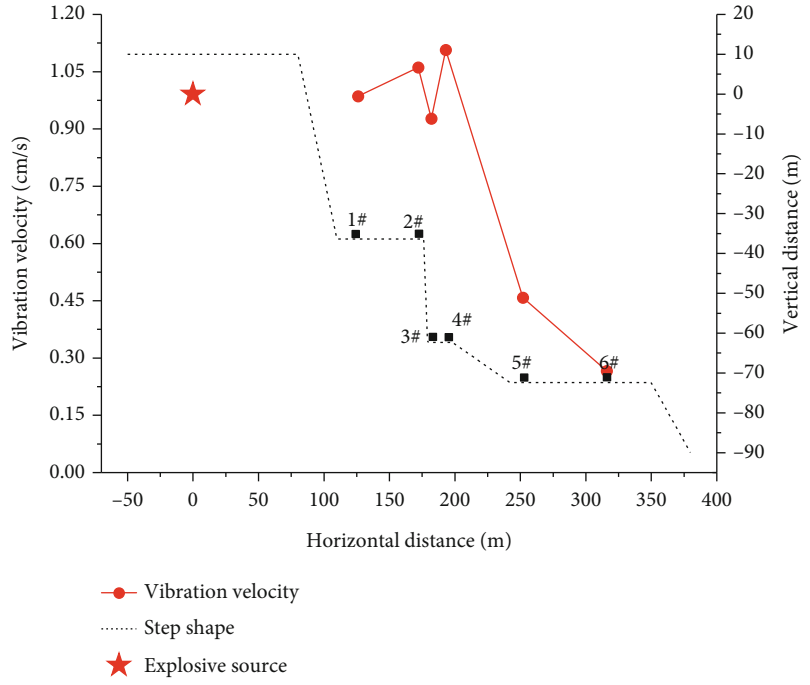

Figure 5: Monitoring data on October 15.

Then, according to Equation (36), Equation (37) is rewritten as

$$V_1 = V \cdot R_{cT} = k\left(\frac{Q^{1/3}}{R}\right)^{\alpha} \cdot k_1 \cdot \left(\frac{1}{H}\right)^{\beta}. \tag{39}$$

Set

$$K = k \cdot k_1. \tag{40}$$

Next, Equation (39) can be rewritten as

$$V_1 = K\left(\frac{Q^{1/3}}{R}\right)^{\alpha} \cdot \left(\frac{1}{H}\right)^{\beta}. \tag{41}$$

Equation (41) is the prediction formula for the negative elevation blasting vibration velocity of the step model. Since R represents the explosion source distance in this formula, the above equation can also be rewritten as

$$V_1 = K\left(\frac{Q^{1/3}}{\sqrt{D^2 + H^2}}\right)^{\alpha} \cdot \left(\frac{1}{H}\right)^{\beta}, \tag{42}$$

where V is the negative elevation step ground particle peak vibration velocity, cm/s; Q is the amount of explosives (the total charge when exploding together, the maximum charge during delayed blasting), kg; D is the horizontal distance from the observation point to the source, m; H is the vertical distance from the observation point to the source, m; k, α are the coefficient and attenuation coefficient associated with the topography and geological conditions between the blasting point and the calculation point. β is the error coefficient

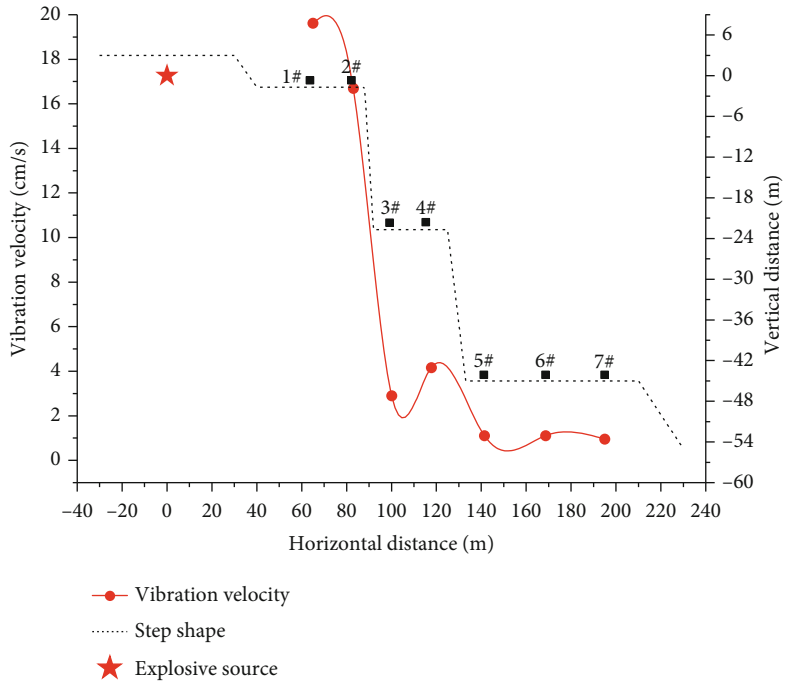

Figure 6: Monitoring data on October 16.

Table 2: Test data regression results.

Formula type	Formula	K	α	β	Cod(r^2)	Reduced chi-sqr	Adj. R-square
Sas (level)	$V = K\left(\sqrt[3]{Q}/D\right)^{\alpha}$	6.43	0.79		0.9806	0.8734	0.9788
Sas (space)	$V = K\left(\sqrt[3]{Q}/\sqrt{D^2+H^2}\right)^{\alpha}$	12912.65	2.75		0.8935	4.7890	0.8838
Improved 1	$V = K\left(\sqrt[3]{Q}/D\right)^{\alpha}\left(\sqrt[3]{Q}/H\right)^{\beta}$	46.16	0.72	0.62	0.9922	0.3860	0.9906
Improved 2	$V = K\left(\sqrt[3]{Q}/\sqrt{D^2+H^2}\right)^{\alpha}\left(\sqrt[3]{Q}/H\right)^{\beta}$	47.28	0.72	0.61	0.9923	0.3796	0.9908
Improved 3	$V = K\left(\sqrt[3]{Q}/\sqrt{D^2+H^2}\right)^{\alpha}\left(H/\sqrt{D^2+H^2}\right)^{\beta}$	47.24	1.34	-0.62	0.9923	0.3796	0.9908
Step (negative)	$V = K\left(\sqrt[3]{Q}/\sqrt{D^2+H^2}\right)^{\alpha}(1/H)^{\beta}$	147.35	0.72	0.62	0.9923	0.3796	0.9908

Notes: (1) Cod(r^2): characterizes the percentage of the variation according to the variable Y, interpreted by the controlled independent variable X; (2) reduced chi-sqr: indicates the degree of the direct difference between the observed and the fitted value; (3) Adj. R-square: the correction coefficient, one of the critical indicators to measure the quality of the model.

associated with the topography and geological conditions between the blasting point and the calculation point.

4. On-Site Blasting Vibration Monitoring Test

Jintuo Coal Mine of Etuoke Banner of Inner Mongolia Autonomous Region (hereinafter referred to as Jinou coal mine) is located in the Heilonggui Mining Area of Qipanjing, Etuoke Banner, Ordos, in the middle of Baiyunwusu Exploration Area of Table Mountain Coalfield, the middle of the 5-6 exploration line of the original exploration area. In the east, the nature zone belongs to the Etuoke flag Albas Sumu. The mining area is nearly 1.4724 km^2, and the mining elevation is 1270~1040 m. The TC-4850 blasting vibrometer manufactured by Chengdu Zhongke Measurement & Control Co., Ltd. was employed in this test. More than 20 blasting vibration tests have been performed since October 2018, and the monitoring data on October 15 and 16 are listed in Table 1.

The data in Table 1 suggests that the distribution law of the vibration velocity with the horizontal distance of the blasting heart can be concluded, as shown in Figures 5 and 6.

Figure 5 shows that compared with 1#, 2#, 3#, and 4# measuring points, the vibration velocity of 2# and 4# measuring points rises; compared with 5# measuring points, particle vibration speed of 4# measuring points decreases significantly.

Table 3: Comparison of calculation accuracy of blasting vibration speed.

Distance (m)		Measured value	Sas (level)		Sas (space)		Improved 1		Improved 1		Improved 1		Step (negative)	
Level	Vertical		Prediction	Error	Prediction	Error	Prediction	Error	Prediction	Error	Prediction	Error	Prediction	Error
126	36.4	0.986	0.607	38.4%	3.124	216.9%	1.819	84.5%	1.842	86.8%	1.809	83.4%	1.793	81.9%
172	36.4	1.061	0.475	55.3%	1.396	31.5%	1.454	37.0%	1.492	40.6%	1.465	38.0%	1.452	36.9%
182	62.3	0.927	0.454	51.0%	1.090	17.5%	1.000	7.9%	1.007	8.7%	0.984	6.1%	0.975	5.2%
193	62.3	1.107	0.433	60.9%	0.942	14.9%	0.959	13.4%	0.970	12.4%	0.947	14.5%	0.939	15.2%
252	72.4	0.458	0.351	23.4%	0.465	1.5%	0.721	57.4%	0.735	60.6%	0.717	56.6%	0.711	55.3%
316	72.4	0.266	0.294	10.3%	0.259	2.5%	0.613	130.3%	0.631	137.3%	0.615	131.4%	0.610	129.4%
65	1.7	19.624	1.024	94.8%	21.514	9.6%	19.580	0.2%	19.787	0.8%	20.033	2.1%	19.864	1.2%
83	1.7	16.696	0.844	94.9%	10.988	34.2%	16.420	1.7%	16.596	0.6%	16.801	0.6%	16.660	0.2%
100	22.7	2.906	0.728	74.9%	6.147	111.5%	2.879	0.9%	2.933	0.9%	2.894	0.4%	2.869	1.3%
117.7	22.7	4.164	0.640	84.6%	4.001	3.9%	2.560	38.5%	2.621	37.0%	2.586	37.9%	2.564	38.4%
141.4	45	1.108	0.554	50.0%	2.225	100.8%	1.468	32.5%	1.481	33.6%	1.451	30.9%	1.439	29.8%
168.6	45	1.114	0.482	56.7%	1.425	27.9%	1.293	16.1%	1.318	18.3%	1.291	15.9%	1.280	14.9%
195	45	0.96	0.430	55.2%	0.977	1.8%	1.165	21.3%	1.194	24.4%	1.170	21.9%	1.160	20.8%
Average relative error				57.73%		44.20%		33.98%		35.54%		33.82%		33.12%

Note: relative error: $|(V_{\text{prediction}}\text{-}V_{\text{measured}})/V_{\text{measured}}| \times 100\%$.

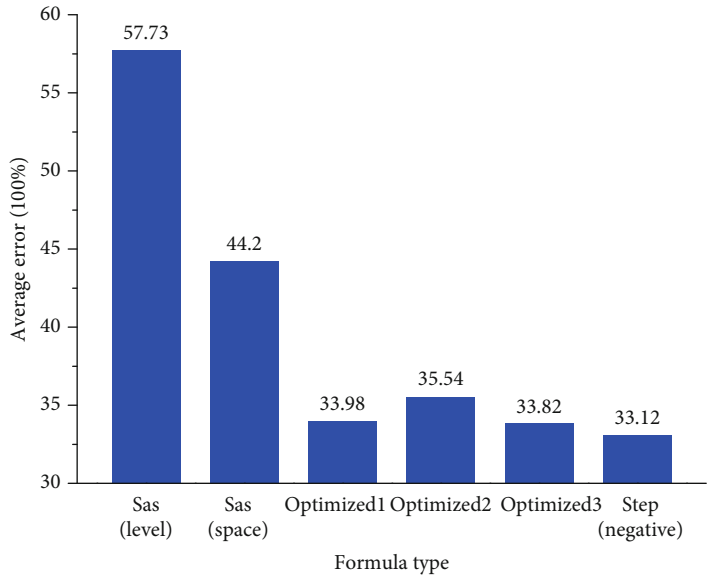

Figure 7: Comparison of prediction accuracy.

Figure 6 suggests that compared with 5#, 6#, and 7# measuring points, the particle vibration speed decreases slowly and keeps basically flat. The difference in vibration speed is the largest between 2# and 3#. Figures 5 and 6 indicate that the vibration velocity of the particle gradually decreases with the rise in the horizontal distance, whereas the existence of the elevation difference leads to a more significant decrease in the vibration velocity of the particle.

5. Discussion

From the above, not only the vibration velocity prediction formula reflecting the negative elevation effect was obtained but also the field measurement of blasting vibration was carried out. Next, in order to test the accuracy of the prediction formula, a regression analysis was performed on the field measured data. Then, the prediction formula obtained in this paper is compared with other improved prediction formulas for error analysis.

5.1. Regression Analysis of Prediction Formula Reflecting Negative Elevation Effect Velocity. Some researchers considered that the commonly used Sadowski formula only considers the vibration velocity V, which decreases as the explosion heart distance R rises, without considering the effect of elevation on the blasting vibration effect.

Accordingly, some optimized formulas are proposed, such as the Sadowski formula (space distance formula) [25].

$$V = K\left(\frac{Q^{1/3}}{\sqrt{D^2 + H^2}}\right)^{a}, \tag{43}$$

where D denotes the horizontal distance between the observation point and the source (m); H is the vertical distance between the observation point and the source. However, literature [26, 27] considers the elevation effect of blasting vibration wave propagation, and the optimized particle vibration velocity prediction formula is written as

$$V = K\left(\frac{Q^{1/3}}{D}\right)^{a}\left(\frac{Q^{1/3}}{H}\right)^{\beta}. \tag{44}$$

Zhu et al. [28] considered that the vibration velocity has an amplifying effect along the elevation, so the calculation of the vibration velocity is defined as

$$V = K\left(\frac{Q^{1/3}}{R}\right)^{a}\left(\frac{Q^{1/3}}{H}\right)^{\beta}, \tag{45}$$

where R denotes the explosion source distance, i.e., the distance between the center of the explosion source and the measuring point (m), which can be written as

$$R = \sqrt{D^2 + H^2}. \tag{46}$$

Tang and Li [29] optimized a calculation formula reflecting the amplifying effect of elevation by the dimensional analysis:

$$V = K\left(\frac{Q^{1/3}}{R}\right)^{a}\left(\frac{H}{R}\right)^{\beta}. \tag{47}$$

The regression analysis was conducted on the above-optimized vibration velocity calculation formula reflecting the elevation effect with Equation (42), and the achieved regression results are listed in Table 2.

Table 2 shows that the Sax (space) formula exhibits the lowest fitting correlation coefficient, the largest degree of difference, and the smallest correction coefficient, indicating that the fitting effect of the formula is the worst. However,

the fitting correlation coefficient, the degree of difference, and the correction determination coefficient of the optimized 2 formula, the optimized 3 formula, and the step (negative) formula are highly consistent with each other.

5.2. Comparison of Blasting Vibration Speed Calculation Accuracy. Based on the regression results achieved in the previous section, the relative error and the average relative error of the monitoring data of Table 1 are compared with the predicted results of the vibration velocity calculation formula reflecting the elevation effect. The comparison results are listed in Table 3 and Figure 7.

Figure 7 suggests that the Sax (horizontal distance) formula exhibits the largest prediction error, reaching 57.73%, followed by the Sa's (space distance) formula, with an error of 44.2%. The step formula (negative) exhibits the smallest error of 33.12%.

6. Conclusion

Aiming at the height effect of bench blasting vibration, this paper uses theoretical research, field measurement, and other methods to carry out research. Established a geometric model of the steps and analyzed the reflection of vibration waves on the free surface of the steps. Conducted on-site monitoring and statistical of blasting vibration. The main conclusions of the paper are as follows:

A vibration propagation model of bench blasting was established, which revealed the mechanism of elevation effect of blasting vibration wave propagating in bench terrain, and provided a more effective new idea for the prediction of blasting vibration.

Based on the reflection theory of elastic waves on a free interface, a calculation formula for predicting the peak vibration velocity of surface particles, the step (negative) formula is proposed. It is found that this formula exhibits a significantly lower error of the prediction results than the commonly used Sa's formula at home and abroad and other optimized formulas.

The feasibility and accuracy of the method to predict the peak velocity of the negative elevation surface in the step blasting project were verified in this study. However, in the positive elevation difference surface and underground blasting engineering, the prediction of the peak velocity of the particle requires further verification.

Data Availability

The test data used to support the findings of this study are included within the article. Readers can obtain data supporting the research results from the test data table in the paper.

Conflicts of Interest

There is no conflict of interest to declare.

Acknowledgments

The study has been supported by the Inner Mongolia Corning Blasting Co., Ltd., the Mining and Metallurgical Technology Group, and the China Blasting Industry Association. Supports from these agencies are gratefully acknowledged. This work was supported by the Major Projects in Inner Mongolia Autonomous Region and the Consulting Research Project of Chinese Academy of Engineering (grant number 2018-XY-12).

References

[1] L. Shuran, J. Yang, L. Guozhen, and Z. Rong, "Study on seismic effect and seismic reduction technology of open pit mine," *Nonferrous Metals (Minerals)*, vol. 3, pp. 30–32, 2003.

[2] S. Daqiang, Y. He, and Z. Dong, "Study on the vibration load of blasting high rock slope and its influence on slope stability," *Engineering Blasting*, vol. 4, pp. 39–43, 1996.

[3] T. Hai and L. Junru, "Numerical simulation of influence of convex geomorphology on blasting vibration wave propagation," *Rock and Soil Mechanics*, vol. 31, no. 4, pp. 1289–1294, 2010.

[4] C. Ming, L. Wenbo, L. Peng, L. Meishan, Z. Chuangbin, and Z. Gen, "Study on the elevation amplification effect of blasting vibration velocity of rock slope," *Chinese Journal of Rock Mechanics and Engineering*, vol. 30, no. 11, pp. 2189–2195, 2011.

[5] W. Pengpeng, Y. Shijie, X. Wenyao, and Y. Qiaomin, "Study on the elevation effect of the velocity of particles in bench blasting," *Blasting*, vol. 32, no. 2, pp. 29–32, 2015.

[6] Z. Weikang, X. Yongsheng, W. Shunchuan, and X. Shu, "Study on the elevation amplification effect of blasting vibration of mine slope," *Metal mine*, vol. 3, pp. 68–71, 2015.

[7] H. Guangqiu, P. Shijie, and L. Xinmin, "Study on the effect of elevation amplification on the vibration attenuation of open pit mining," *Gold*, vol. 36, no. 7, pp. 28–32, 2015.

[8] Z. Tongling and L. Yushou, "The formula of blasting vibration reflecting elevation and its application," *Jiangsu Coal*, vol. 4, pp. 19-20, 1997.

[9] F. Bo, H. Yingguo, L. Wenbo, C. Ming, and Y. Peng, "Analysis of local amplification effect of blasting vibration of high rock slope," *Blasting*, vol. 31, no. 2, pp. 1–7, 2014.

[10] L. Shiyan, L. Changhong, Q. Lan, and L. Baoxu, "Numerical simulation of influence of blasting vibration on highway slope," *Journal of University of Science and Technology Beijing*, vol. 6, pp. 507–509, 2003.

[11] Y. G. Zhang, J. Tang, R. P. Liao et al., "Application of an enhanced BP neural network model with water cycle algorithm on landslide prediction," *Stochastic Environmental Research and Risk Assessment*, 2020.

[12] Y. Zhang, J. Tang, Z. Y. He, J. Tan, and C. Li, "A novel displacement prediction method using gated recurrent unit model with time series analysis in the Erdaohe landslide," *Natural Hazards*, vol. 105, no. 1, pp. 783–813, 2021.

[13] Y. Zhang and L. Yang, "A novel dynamic predictive method of water inrush from coal floor based on gated recurrent unit model," *Natural Hazards*, vol. 105, no. 1, pp. 2027–2043, 2020.

[14] Y. G. Zhang, Z. Zhang, S. Xue, R. Wang, and M. Xiao, "Stability analysis of a typical landslide mass in the Three Gorges Reservoir under varying reservoir water levels," *Environmental Earth Sciences*, vol. 79, no. 1, 2020.

[15] Y. G. Zhang, S. Zhu, J. Tan, L. Li, and X. Yin, "The influence of water level fluctuation on the stability of landslide in the Three

Gorges Reservoir," *Arabian Journal of Geosciences*, vol. 13, no. 17, p. 845, 2020.

[16] Y. Zhang, S. Zhu, W. Zhang, and H. Liu, "Analysis of deformation characteristics and stability mechanisms of typical landslide mass based on the field monitoring in the Three Gorges Reservoir, China," *Journal of Earth System Science*, vol. 128, no. 1, 2019.

[17] B. Gong, Y. Jiang, P. Yan, and S. Zhang, "Discrete element numerical simulation of mechanical properties of methane hydrate-bearing specimen considering deposit angles," *Journal of Natural Gas Science and Engineering*, vol. 76, article 103182, 2020.

[18] B. Gong, Y. Jiang, and L. Chen, "Feasibility investigation of the mechanical behavior of methane hydrate- bearing specimens using the multiple failure method," *Journal of Natural Gas Science and Engineering*, vol. 69, article 102915, 2019.

[19] J. Lu, *Principles of Seismic Exploration (Volume 2)*, China University of Petroleum Press, Shandong Dongying, 1993.

[20] L. Xiwu, *The Basis of Elastic Wave Field Theory*, China Ocean University Press, Qingdao, 2008.

[21] Y. Qiaoming, Y. Shijie, X. Wenyao, W. Pengpeng, and W. Jing, "Study on the amplification effect of blasting seismic waves at the top of the step slope," *Modern Mining*, vol. 31, no. 1, pp. 40-41, 2015.

[22] G. Guillaume, J. Picaut, G. Dutilleux, and B. Gauvreau, "Time-domain impedance formulation for transmission line matrix modelling of outdoor sound propagation," *Journal of Sound & Vibration*, vol. 330, no. 26, pp. 6467–6481, 2011.

[23] X. Zhengxue, Z. Zhicheng, and L. Chaoding, *Dynamics and Seismic Effects of Blasting Seismic Waves*, University of Electronic Science and Technology of China Press, Chengdu, 2004.

[24] L. Wang, *Stress Wave Foundation (2nd Edition)*, National Defence Industry Press, Beijing, 2005.

[25] H. Xuelong, Q. Shijie, J. Wenli et al., "Attenuation law of blasting seismic wave based on equivalent path," *Explosion and Shock Wave*, vol. 37, no. 6, pp. 966–975, 2017.

[26] M. Jifu and H. Hongbin, *Blasting Test Technology*, Metallurgical Industry Press, Beijing, 1992.

[27] National Development and Reform Commission of the People's Republic of China, *SL-94 Technical Specifications for Construction of Rock Foundation Excavation of Hydraulic Structures*, Water Resources and Hydropower Press, Beijing, 1994.

[28] Z. Zhu, L. Honggen, and M. Jinwei, "Selection of the law of seismic wave propagation along slopes," *Blasting*, vol. 2, pp. 30-31, 1988.

[29] T. Hai and L. Hai-bo, "Study of blasting vibration formula reflecting elevation amplification effect," *Rock and Soil Mechanics*, vol. 32, no. 3, pp. 820–824, 2011.